

# Mainz Microtron MAMI

**Collaboration:** A1

**Spokesperson:** H. Merkel

**Title:** Measurements of the elastic electron-proton cross section and separation of the form factors  $G_e$  and  $G_m$  in the  $Q^2$  region from 0.1 (GeV/c)<sup>2</sup> to 2 (GeV/c)<sup>2</sup>

**Authors:** P. Achenbach<sup>1</sup>, C. Ayerbe<sup>1</sup>, D. Baumann<sup>1</sup>, J. C. Bernauer<sup>1</sup>, R. Böhm<sup>1</sup>, D. Bosnar<sup>4</sup>, M. O. Distler<sup>1</sup>, L. Doria<sup>1</sup>, J. Friedrich<sup>1</sup>, W. Heil<sup>2</sup>, P. Jennewein<sup>1</sup>, J. Krimmer<sup>2</sup>, K. W. Krygier<sup>1</sup>, M. Makek<sup>4</sup>, H. Merkel<sup>1</sup>, U. Müller<sup>1</sup>, R. Neuhausen<sup>1</sup>, L. Nungesser<sup>1</sup>, J. Pochodzalla<sup>1</sup>, M. Potokar<sup>3</sup>, S. Sánchez Majos<sup>1</sup>, S. Širca<sup>3</sup>, Th. Walcher<sup>1</sup>, M. Weinriefer<sup>1</sup>

<sup>1</sup> Institut für Kernphysik, Universität Mainz, Germany

<sup>2</sup> Institut für Physik, Universität Mainz, Germany

<sup>3</sup> Institut "Jožef Stefan", Ljubljana, Slovenia

<sup>4</sup> Department of Physics, University of Zagreb, Croatia

**Contactperson:** M. O. Distler

**Abstract of physics:** We propose to perform a high precision measurement of the elastic cross section in the reaction  $H(e, ep)$  in the complete accessible range.

**Abstract of equipment:** Additionally to the standard equipment, we want to install a remote control for the spectrometer position.

## MAMI specifications :

beam energy:	min. 180 MeV	max. 1530 MeV
beam current:	min. 25 pA	max. 15 $\mu$ A
time structure:	continuous beam	
polarization:	no	

## Experiment specifications :

hall:	spectrometer hall		
beam line:	standard to spectrometer hall		
spectrometer:	particles:	range of angles:	out of plane:
A	e	18° – 160°	0°
B	e,p	7° – 62°	0°
C	e	18° – 160°	0°
special detectors:	none		

## Beam time request : 502h

set-up without beam:	4 days
set-up with beam:	182 hours
data taking:	320 hours

# Measurements of the elastic electron-proton cross section and separation of the form factors $G_e$ and $G_m$ in the $Q^2$ region from $0.1 \text{ (GeV/c)}^2$ to $2 \text{ (GeV/c)}^2$

Patrick Achenbach<sup>1</sup>, Carlos Ayerbe Gayoso<sup>1</sup>, Dagmar Baumann,<sup>1</sup> Jan C. Bernauer<sup>1</sup>,  
Ralph Böhm<sup>1</sup>, Michael O. Distler<sup>1</sup>, Luca Doria<sup>1</sup>, Jörg Friedrich<sup>1</sup>, Werner Heil<sup>2</sup>,  
Peter Jennewein<sup>1</sup>, Jochen Krimmer<sup>2</sup>, Klaus Werner Krygier<sup>1</sup>, Harald Merkel<sup>1</sup>,  
Ulrich Müller<sup>1</sup>, Reiner Neuhausen<sup>1</sup>, Lars Nungesser<sup>1</sup>, Josef Pochodzalla<sup>1</sup>, Salvador Sánchez,<sup>1</sup>  
Thomas Walcher<sup>1</sup>, Markus Weinriefer<sup>1</sup>  
(<sup>1</sup>*Institut für Kernphysik*, <sup>2</sup>*Institut für Physik, Universität Mainz, Germany*)

Milan Potokar, Simon Širca  
(*Institut "Jožef Stefan", Ljubljana, Slovenia*)

Damir Bosnar, Mihael Makek  
(*Department of Physics, University of Zagreb, Croatia*)

We request 502 hours of beam time to perform a high precision measurement of the elastic cross section in the reaction  $H(e, ep)$  in the complete accessible range. The form factors  $G_e$  and  $G_m$  will be analyzed using two approaches. On the one hand, they will be extracted using a fit of several ansätze to the measured cross sections. On the other hand, a Rosenbluth separation will be performed. The results will be examined with regard to a pion cloud contribution. The bulk of the beam time will be used for calibrations, in particular for the determination of the efficiencies of the detectors and the remeasurement of the transfer matrices of the spectrometers. For the latter of these, a new algorithm with spline functions will be used.

# 1 Introduction and Motivation

The form factors of the proton encode unique information about the proton's internal structure, provided they are determined with sufficient precision. The Fourier transform of the form factors in the Breit frame yields the spatial distribution of the charge and magnetization, providing important insight into the constituents of the proton, their interaction and wave functions. The replication of the form factors by a model of the proton is a significant test of its validity.

In absence of two photon exchange, the elastic cross section on a spin- $\frac{1}{2}$ -particle is given by the Rosenbluth-formula [Ros50]:

$$\frac{d\sigma}{d\Omega} = \left( \frac{d\sigma}{d\Omega} \right)_{Mott} \cdot \frac{1}{\epsilon(1+\tau)} (\tau G_m^2 + \epsilon G_e^2), \quad (1)$$

where  $\tau = Q^2/4m_p^2$ ,  $\epsilon$  is the longitudinal polarization of the exchanged virtual photon  $\epsilon = (1 + 2(1 + \tau) \tan^2 \frac{\theta}{2})^{-1}$ ,  $m_p$  is the mass of the target particle, i.e. the mass of the proton, and  $\theta$  is the electron scattering angle.

The cross section is thus a function of the two form factors  $G_e$  and  $G_m$ , which can be extracted as functions of  $Q^2$  by measurements at constant  $Q^2$  but different  $\epsilon$ , a so called Rosenbluth separation. An alternative procedure consists of a fit of a sufficiently flexible model ansatz for  $G_e$  and  $G_m$ .

New interest in the proton form factor has been stimulated by a precise measurement of the proton radius via Laser spectroscopy [Kar99]. Their quite large rms-radius of 0.890 fm came as a surprise to those who still believe in the old Stanford value of 0.805 fm [HMW63] or who believed in the standard dipole fit (which yields a comparable value) as a perfect description of the nucleons. On the other hand, with the old Mainz data [BPS<sup>+</sup>74, SSBW80], there existed a very accurate measurement with the result  $r_{p,e} = 0.857 \pm 0.008$  fm and  $r_{p,m} = 0.83 \pm 0.07$  fm. Therefore, we did not see the necessity to remeasure the proton radius in light of the laser spectroscopy result.

New interest however has arisen due to recent  $G_{e,p}$ -measurements with polarization experiments [M<sup>+</sup>98, P<sup>+</sup>01, G<sup>+</sup>02], which, at  $Q^2$  beyond 1 (GeV/c)<sup>2</sup>, revealed drastic deviations from the dipole fit. Recent results for  $G_{e,n}$  (also from polarization measurements), together with the new situation for  $G_{e,p}$  led Friedrich and Walcher to have a closer look at the nucleon form factors [FW03]. They analyzed all four standard nuclear form factors ( $G_{e,p}, G_{e,n}, G_{m,p}, G_{m,n}$ ) with the same phenomenological ansatz (eq. 2); the sum of a smooth part,  $G_s$  (eq. 3), described by two dipoles, and a bump,  $G_b$  (eq. 4):

$$G_N = G_s + a_b Q^2 \cdot G_b \quad (2)$$

$$G_s = \frac{a_{10}}{\left(1 + \frac{Q^2}{a_{11}}\right)^2} + \frac{1 - a_{10}}{\left(1 + \frac{Q^2}{a_{21}}\right)^2} \quad (3)$$

$$G_b = \left( e^{-\frac{1}{2} \left(\frac{Q-Q_b}{\sigma_b}\right)^2} + e^{\frac{1}{2} \left(\frac{Q+Q_b}{\sigma_b}\right)^2} \right) \quad (4)$$

This ansatz, which holds for all four form factors, reveals a bump/dip around  $Q^2 = 0.2$  (GeV/c)<sup>2</sup>, as shown for the proton form factors by the deviation of the existing data from the smooth part (eq. 3), shown in figure 1.

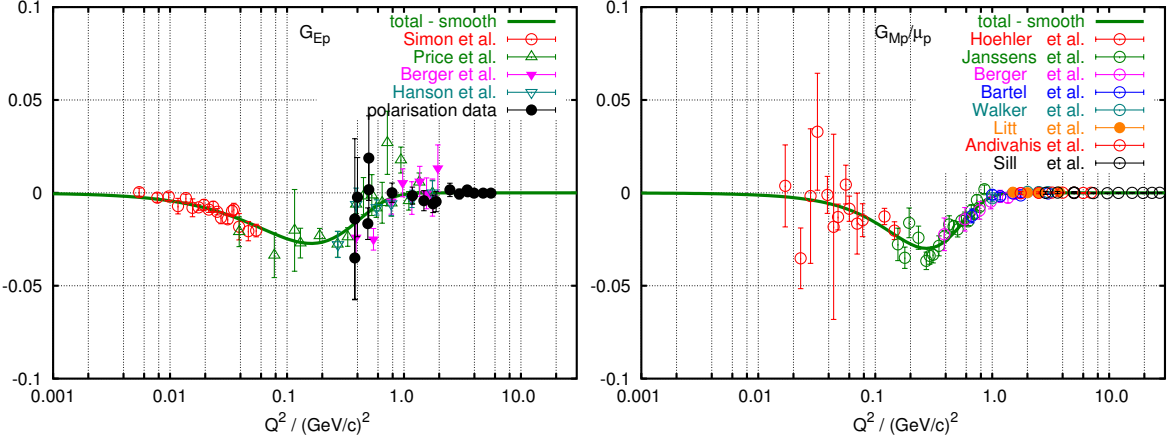


Figure 1: The difference between the measured form factors  $G_{e,p}$  and  $G_{m,p}$  and the smooth part (eq. 3) of the phenomenological ansatz.

Additionally, the authors proposed a physically motivated ansatz. The nucleons are described by a sum of a bare nucleon plus a polarization part, for the proton:

$$p = (1 - b_p) p^0 + b_p (n^0 + \pi^+).$$

The bare nucleons are interpreted in terms of constituent quarks, which are described with a dipole form for each quark

$$G^{qN} = \frac{a_0^{qN}}{(1 + Q^2/a_1^{qN})^2}. \quad (5)$$

The polarization term consists of a pion cloud contribution with the form factor of a 1p-wave

$$G^\pi = a_0^\pi \cdot \left(1 - \frac{1}{6} (Q/a_1^\pi)^2\right) e^{-\frac{1}{4} (Q/a_1^\pi)^2}, \quad (6)$$

and a corresponding contribution of the “complementary” bare nucleon.

The electric form factor of the proton thus reads

$$G_{e,p} = (G_E^{up} + G_E^{dp}) (1 - b_p) + b_p \left( (G_E^{un} + G_E^{dn}) + G_E^{\pi^+} \right). \quad (7)$$

The  $a_0^{qN}$  are given by the quark charges, therefore six free parameters remain in this ansatz. For the magnetic form factor, the translation from the constituent quark model is not that straight forward (For details, see [FW03]). Therefore, the ansatz for  $G_m$  consists of two dipoles (one long range,  $G_{\text{Dipole}}^{\text{out}}$ , and one short range,  $G_{\text{Dipole}}^{\text{in}}$ ) and the pion cloud contribution:

$$G_{m,p} = G_{\text{Dipole}}^{\text{out}} + G_{\text{Dipole}}^{\text{in}} + G^\pi. \quad (8)$$

This, too, gives six parameters.

The data currently available ranges from 0.01 to over 8.8  $(\text{GeV}/c)^2$  for  $G_{e,p}$ , and from 0.02 to over 31  $(\text{GeV}/c)^2$  for  $G_{m,p}$  (an overview can be found in [FW03]). However, figure 1

shows that, over the interesting bump region around  $0.2 \text{ (GeV/c)}^2$ , measurements from many laboratories contribute. Though the different datasets agree surprisingly well, it is important to establish this bump structure in an internally coherent measurement with high precision. MAMI and the magnetic spectrometers of the A1-collaboration are the ideal facility for this purpose. We propose to measure the elastic electron-proton cross section with a precision of 0.5% or better in the  $Q^2$ -region that our instruments can access, i.e. from 0.1 to  $2 \text{ (GeV/c)}^2$ .

## 2 Accessible kinematic region and chosen settings

The kinematics setup of an elastic scattering experiment is described completely by any two parameters from the set  $\{\epsilon, Q^2, E, E', \theta\}$ . For the analysis, the most practical combination is  $Q$  and  $\epsilon$ , because the form factors depend on  $Q^2$  and the accessible  $\epsilon$ -region defines the lever arm for a separation in the sense of the Rosenbluth-formula.

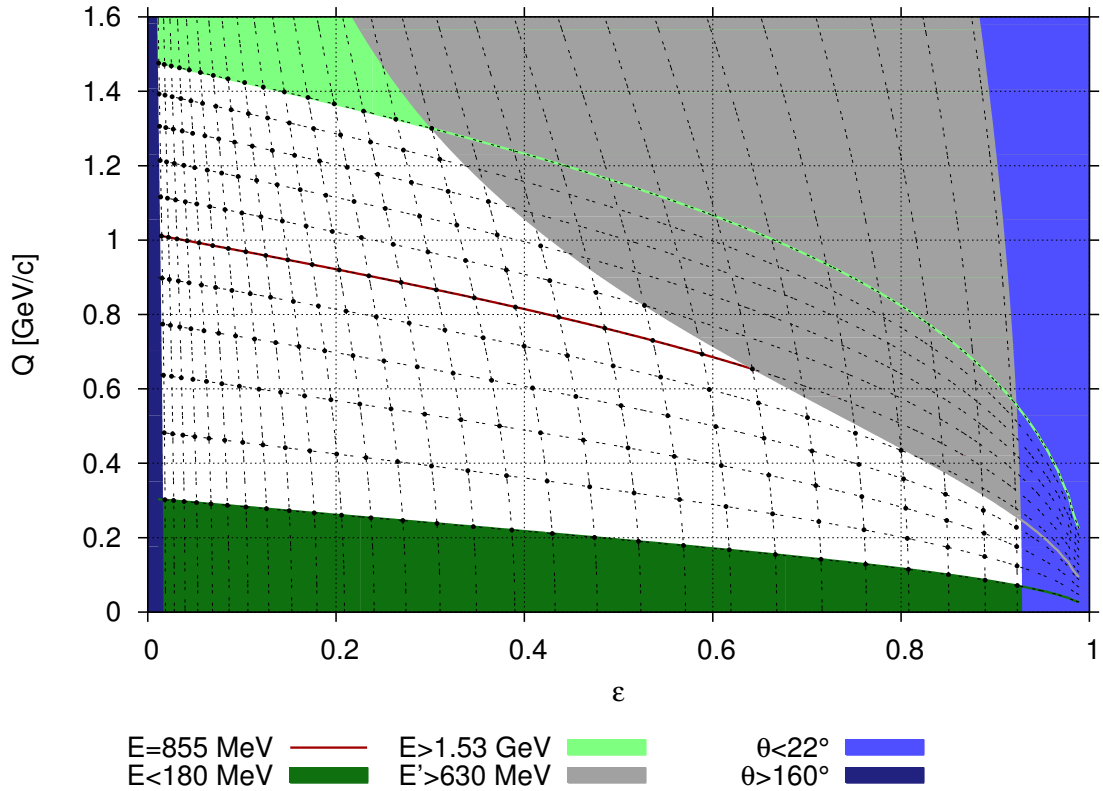


Figure 2: The accessible kinematic region in  $\epsilon/Q$ -space. The black dots represent the chosen settings (centers of the respective acceptance). The dotted curves correspond to constant incident beam energies in steps of 135 MeV (“horizontal” curves) and to constant scattering angles in  $5^\circ$  steps (“vertical” curves). Also shown are the limits of the facility: The red line represents the current accelerator limit of 855 MeV, with the upgrade, it will be possible to measure up to the light green curve. The dark (light) blue area shows the kinematic region excluded from measurement due to the maximum (minimum) possible spectrometer angle. The gray shaded region is excluded by the upper momentum of spectrometer A (630 MeV/c).

The accessible region is defined through the accelerator and the properties of the detector system. Figure 2 shows the accessible region for an experiment with spectrometer A of the A1-collaboration.

The upper end of the accessible  $Q$  region is set by the maximum incident beam energy. MAMI B provides an electron beam with energies up to 855 MeV; the corresponding limit is drawn as a red line in the figure. The extension of MAMI (MAMI C), will raise the maximum beam energy to over 1.5 GeV, raising the limit in  $Q$  to over 1.4 GeV/c (light green area). The lower end is given by the lower limit of the incident beam energy (180 MeV, dark green area).

The maximum possible scattering angle determines the lower end of the  $\epsilon$  region. The maximum backward angle of spectrometer A is  $160^\circ$ , which excludes the dark blue area. The minimum angle is  $22^\circ$ , setting the higher end of the  $\epsilon$  region (light blue). A future upgrade of the exit dipole with a water cooling system will lower the minimum angle by a small amount, so additional measurements may be possible.

Spectrometer A has a maximum central momentum of 630 MeV/c. This excludes measurements at higher beam energies and forward angles (gray area).

The angular acceptance of spectrometer A is a little wider than  $\pm 5^\circ$ , thus a spacing of  $5^\circ$  between the settings gives about 50% overlap to allow checks for systematic errors. In Figure 3, the acceptances for the five setups with the central angles of  $43^\circ$ ,  $48^\circ$ ,  $53^\circ$ ,  $58^\circ$  and  $63^\circ$  at 585 MeV incident beam energy are shown. While the acceptance in  $q$  and  $\theta$  of the spectrometer itself forms essentially a quadrangle, this is reduced to a simple curve both in  $\epsilon/Q$ - and  $\theta/Q$ -space, since  $\epsilon$  and  $Q$  are functions of  $E$  and  $\theta$ . In figure 2, the acceptance of one setting covers a piece of the black “horizontal” curves, from the neighbouring settings.

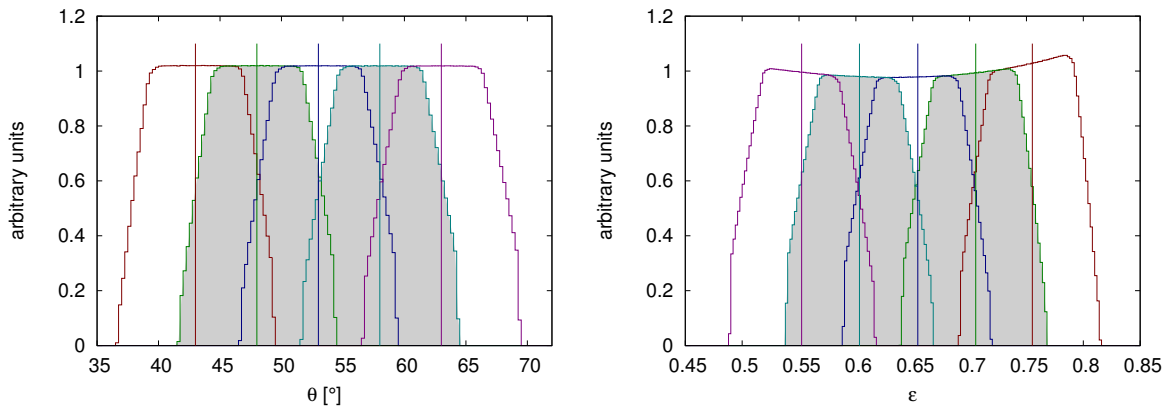


Figure 3: The acceptance for five setups at 585 MeV incident beam energy in  $\theta$  (left) and  $\epsilon$  (right). The vertical lines represent the central angles of  $43^\circ$ ,  $48^\circ$ ,  $53^\circ$ ,  $58^\circ$  and  $63^\circ$  and the corresponding  $\epsilon$  values. For every angle/ $\epsilon$ , at least two settings contribute.

The accelerator can only provide discrete levels of energy with a spacing of 15 MeV (for the existing system), and the change of the energy is quite time consuming and thus prohibitive to be done for every setting, therefore, it is best to select a few fixed energies. We choose constant intervals of 135 MeV, which is a trade-off between time and number of setups. The energy upgrade is still under construction, and the design of the ejection system has not yet been finalized. Thus, the energies above 0.855 GeV are preliminary and subject to change.

The resulting setups form a rectangular equidistant grid in the  $E/\theta$ -Space, with 135 MeV spacing in  $E$  and  $5^\circ$  in  $\theta$ . This translates to the black dots in figure 2.

It is possible in the future to measure at smaller scattering angles and higher electron energies with the KaoS spectrometer [CRC04], but this is not in the scope of this proposal.

### 3 Experimental requirements

The standard setup of the three-spectrometer facility at MAMI will be used [B<sup>+</sup>98]. Due to the large number of setups, a hall access for every setup change adds a large overhead. Thus we suggest to install a remote control of the spectrometer positioning. This will reduce the overhead to the time needed to set the magnetic field. An unpolarized beam current of 25pA to  $15\mu\text{A}$  will be used. We will use a liquid hydrogen target with the standard extended target cell of the A1-collaboration [Ewa96]. Spectrometer A will be configured to measure the scattered electrons, spectrometer B will detect the recoil protons (see next chapter). Additionally, in some settings, the electron will be measured with spectrometer B in order to achieve control of systematic uncertainties. Spectrometer C will be used to monitor the luminosity constancy.

### 4 Error control

Due to the construction of spectrometer A, elastic scattering essentially results in a line on the detector system along which the events are spread out according to the scattering angle, or, equivalently,  $Q$ . Thus, the local efficiency of the detectors has to be well understood. To this end, for some settings the recoil proton will be measured in coincidence with spectrometer B (recording all single events in both spectrometers). This “tagging” permits the determination of the local efficiency from the measured single/coincident events ratio. We are confident, that this, together with the redundant measurements with 50% overlap and the techniques developed in [Ber04], will reduce the influence of these inefficiencies such that they are irrelevant.

To control the beam properties (luminosity, position), we will use spectrometer C. It will measure the electrons at rather large backward angles with only a few setup changes over the whole time.

A new beam stabilization system has been constructed for the A1 beam line by the B1 collaboration (a comparable system is already used by the A4 collaboration “parity violating electron scattering”). This will reduce the influence of beam instabilities so that they are negligible.

Since about 30 of our settings will be measured at 180 MeV, i.e. using only RTMs 1 and 2, it is essential that some remaining issues with beam stability at that energy will be resolved by the accelerator group.

In [Ber04], a new method for the determination of the transfer functions of the spectrometers was developed. It uses a spline-based expansion and yields a better reconstruction of the target coordinates (30% smaller missing mass peaks). We want to employ that technique in the proposed experiment. For that, we need some beam time with the moving  $^{12}\text{C}$  target constructed in the forementioned diploma thesis.

## 5 Method of analysis, error estimates

The beam time for each measurement is determined by the following considerations:

- Maximum current is  $15 \mu A$ . This will limit the beam spot size and the risk of a boiling target.
- Maximum counting rate is 300 Hz, to limit the dead time.
- Minimal measuring time per setup is 30 minutes, to get accurate dead time estimations.
- Times are rounded up to the next multiple of 10 minutes.
- The statistical error should be  $< 0.5\%$  (for the whole acceptance)

We estimate the errors in the cross section measurements by the statistical error plus a margin of 0.5% for unaccounted, but setup dependent errors, like deviations in the magnetic field, transfer matrix and angular position of the spectrometer. This leads to an error of 1% or less in every cross section measurement. A further increase in beam time for each setting will most likely be futile, since the statistical error would become irrelevant in relation to these other effects.

### 5.1 Rosenbluth-Separation

The standard way to analyse this kind of measurement is to separate the form factors by a Rosenbluth separation. Exploiting the linear form of eq. 1, one can separate  $G_m$  and  $G_e$  at any given  $Q^2$  by measuring several settings at constant  $Q^2$  but different  $\epsilon$ . This works in a completely model independent way, as long as eq. 1 holds true. This might not be the case for larger  $Q^2$ , when the two photon exchange contribution becomes larger [GV03]. Additionally, to be truly model independent, one has to accept only a very small region around the targeted  $Q^2$  value.

With the estimated errors in the cross section, one can create pseudo data and determine the errors in the resulting  $G_e$ ,  $G_m$ . This yields an error of about 1% in the extracted form factors. The method itself is not robust against normalization problems. One can check for these kind of problems by extrapolating to  $Q = 0$  and comparing to the known values  $G_{e,p}(Q^2 = 0) = 1$  and  $G_{m,p}(Q^2 = 0) = \mu_p$ , but this requires a model to be applied, loosing or at least softening the biggest advantage of this method. Measurements for several  $\epsilon$  are needed to determine the linearity of the Rosenbluth plot as a test of the validity of the one-photon-exchange assumption in the respective  $Q^2$ -range. In the proposed experiment, the number of different  $\epsilon$ -values for a given  $Q$  varies between 2 and 4, so that additional measurements for selected  $Q$ -values may be needed in the future.

### 5.2 Global Fit

A superior approach is to fit a global ansatz for the form factors directly to the cross sections. With a flexible ansatz, this is quasi model-independent. This approach, however, is an even more powerful method to test given models directly.

For an error estimate, again, a Monte-Carlo calculation has been performed. Starting from the phenomenological fit of Friedrich / Walcher described above, many data-sets consisting of

pseudo data with errors for all settings of the proposed experiment were generated. A global efficiency factor of 0.95 was taken into account here, a value much smaller than we expect for the A1 detector systems.

### 5.2.1 Phenomenological fit

A fit with the phenomenological ansatz and free normalization has now been done for every data-set. The normalization parameter is reproduced with an error estimate of 0.3%, so the global efficiency in the experiment will not affect the analysis in a critical way. The reproduced  $G_{e/m}$ -curves are shown in figure 4.

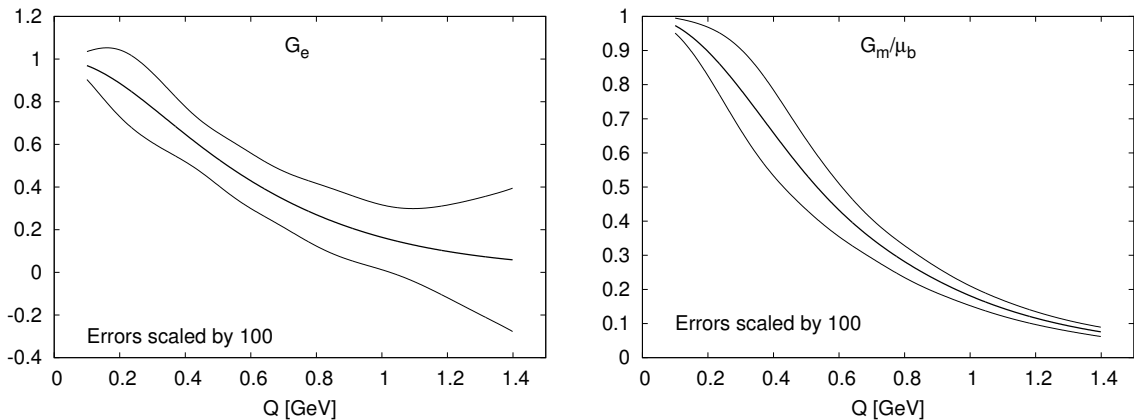


Figure 4:  $G_e$  (left) and  $G_m$  (right) of the phenomenological ansatz and anticipated errors from the proposed experiment (the thinner lines represent the estimated  $1\sigma$ -errors). The errors are scaled by a factor of 100.

Physically, the bump structure term

$$a_b Q^2 G_b(Q^2; Q_b, \sigma_b) \quad (9)$$

is very interesting. Figure 5 shows the predicted errors on that part. Since the contribution of this term is very small, the relative errors are naturally a lot larger. The estimated errors are, none the less, small enough to permit the extraction of the bump parameters.

### 5.2.2 Physically motivated ansatz

In the same manner, error estimates for an analysis with the physically motivated ansatz are calculated. The results for the complete form factors are shown in figure 6, those for the pion cloud contribution in figure 7. The achievable error is small enough to be informative about the pion cloud contribution.

### 5.2.3 Additional data and theoretical models

If the data available up to now, especially for larger  $Q$ , are also taken into account, the errors will be further reduced, particularly since the “smooth part”, i.e. the dipoles, will be better fixed. Besides the models shown above, it is possible to fit any function to the cross section that anyone can come up with, for example a model including two-photon-exchange.

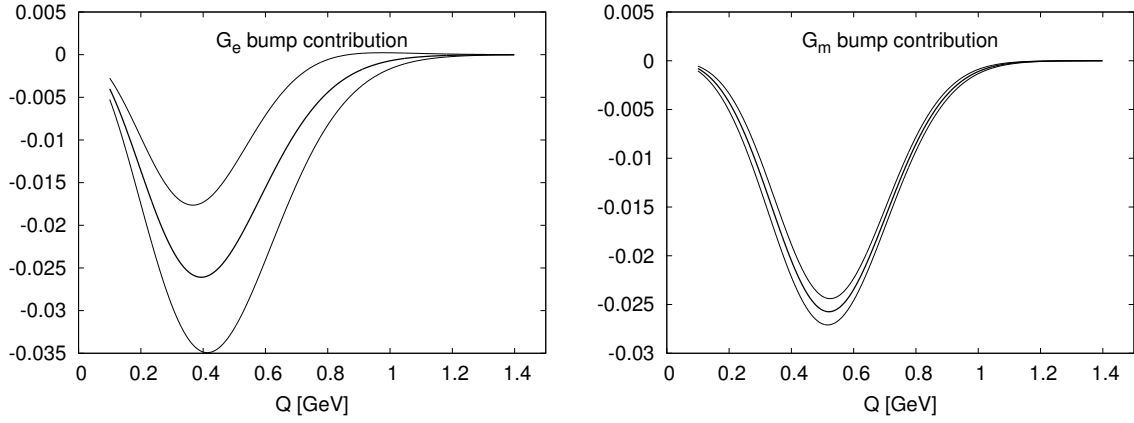


Figure 5: Extracted bump contribution (eq. 9) to  $G_e$  (left) and  $G_m$  (right). The thin lines show the anticipated errors.

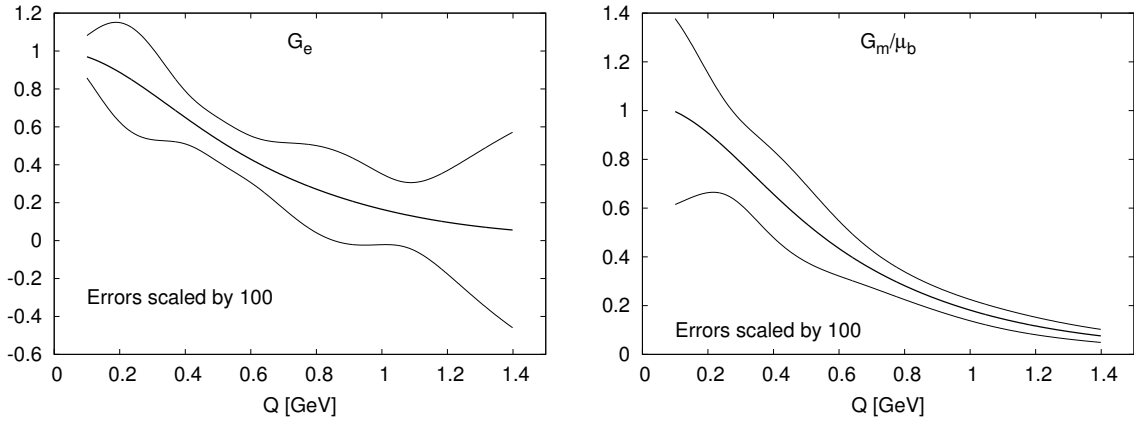


Figure 6:  $G_e$  (left) and  $G_m$  (right), as extracted with the physically motivated ansatz.

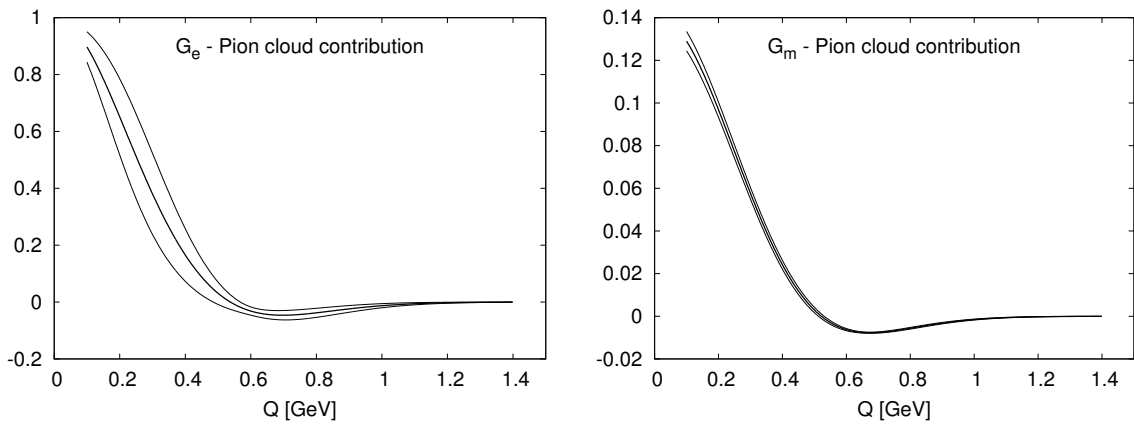


Figure 7: Pion-cloud contribution to  $G_e$  (left) and  $G_m$  (right).

## 6 Beam time request

We request 502 hours of beam-time, according to the following schedule

- 246 setups with durations between 30 and 80 minutes: 130h
- 246 setup changes of about 15 min: 62h
- overhead for overlapping and additional control measurements: 50h
- 10 beam energy changes: 60h
- $\sim 1$  week for the measurement of the transfer matrices of all 3 spectrometers: 140h
- $\sim 3$  days (20h per day) for calibration runs: 60h

Additionally, we require about 4 days without beam for the installation of the moving  $^{12}\text{C}$  target and the liquid hydrogen target system.

## 7 Possible experiment without MAMI C

Without the energies provided by MAMI C, only about half of the setups can be measured. For this, 380 hours of beam-time will be needed. Since the data at higher  $Q$  is missing, the dipoles will not be determined as accurately. However, the pion cloud contribution in the physically motivated ansatz would be determined to a satisfactory level. Together with the existing data, in particular at higher  $Q^2$ , it would be possible to extract the bump structure in the phenomenological ansatz even with such a reduced measurement program.

We propose to measure in two parts: Firstly, we want to measure the energies up to 0.855 GeV and secondly, when MAMI C has been completed, we will measure the remaining energies in a further beam time period. The additional data will provide a much better control of the systematic errors and will allow us to select ansätze with a higher degree of freedom.

## 8 List of planned setups

E [GeV]	$\theta$ [°]	q [GeV/c]	$\epsilon$	time [min]
0.180	158	0.302	0.0181	30
0.180	153	0.300	0.0273	30
0.180	148	0.297	0.0386	30
0.180	143	0.294	0.0518	30
0.180	138	0.291	0.0671	30
0.180	133	0.287	0.0846	30
0.180	128	0.283	0.1042	30
0.180	123	0.278	0.1261	30
0.180	118	0.273	0.1502	30
0.180	113	0.267	0.1768	30
0.180	108	0.260	0.2057	30
0.180	103	0.254	0.2370	30
0.180	98	0.246	0.2708	30
0.180	93	0.238	0.3071	30
0.180	88	0.230	0.3457	30
0.180	83	0.221	0.3865	30
0.180	78	0.211	0.4295	30
0.180	73	0.201	0.4745	30
0.180	68	0.190	0.5210	30
0.180	63	0.179	0.5689	30
0.180	58	0.167	0.6175	30
0.180	53	0.155	0.6664	30
0.180	48	0.142	0.7149	30
0.180	43	0.129	0.7623	30
0.180	38	0.115	0.8077	30
0.180	33	0.101	0.8503	30
0.180	28	0.086	0.8892	30
0.180	23	0.071	0.9234	30
0.315	158	0.482	0.0174	30
0.315	153	0.479	0.0263	30
0.315	148	0.476	0.0372	30
0.315	143	0.472	0.0500	30
0.315	138	0.467	0.0649	30
0.315	133	0.462	0.0818	30
0.315	128	0.456	0.1010	30
0.315	123	0.449	0.1224	30
0.315	118	0.442	0.1461	30
0.315	113	0.434	0.1721	30
0.315	108	0.425	0.2007	30
0.315	103	0.415	0.2317	30
0.315	98	0.404	0.2653	30
0.315	93	0.393	0.3014	30
0.315	88	0.380	0.3399	30
0.315	83	0.367	0.3809	30
0.315	78	0.352	0.4241	30

E [GeV]	$\theta$ [°]	q [GeV/c]	$\epsilon$	time [min]
0.315	73	0.337	0.4694	30
0.315	68	0.320	0.5164	30
0.315	63	0.303	0.5648	30
0.315	58	0.284	0.6140	30
0.315	53	0.264	0.6636	30
0.315	48	0.243	0.7127	30
0.315	43	0.221	0.7607	30
0.315	38	0.198	0.8066	30
0.315	33	0.174	0.8496	30
0.315	28	0.150	0.8888	30
0.315	23	0.124	0.9232	30
0.450	158	0.637	0.0167	30
0.450	153	0.634	0.0252	30
0.450	148	0.630	0.0356	30
0.450	143	0.625	0.0480	30
0.450	138	0.620	0.0623	30
0.450	133	0.614	0.0787	30
0.450	128	0.607	0.0972	30
0.450	123	0.599	0.1180	30
0.450	118	0.591	0.1411	30
0.450	113	0.581	0.1666	30
0.450	108	0.571	0.1946	30
0.450	103	0.559	0.2251	30
0.450	98	0.546	0.2583	30
0.450	93	0.532	0.2942	30
0.450	88	0.517	0.3326	30
0.450	83	0.500	0.3736	30
0.450	78	0.482	0.4170	30
0.450	73	0.463	0.4626	30
0.450	68	0.441	0.5101	30
0.450	63	0.419	0.5592	30
0.450	58	0.394	0.6092	30
0.450	53	0.368	0.6595	30
0.450	48	0.340	0.7095	30
0.450	43	0.310	0.7583	30
0.450	38	0.279	0.8049	30
0.450	33	0.246	0.8485	30
0.450	28	0.212	0.8882	30
0.450	23	0.176	0.9229	30
0.585	158	0.774	0.0159	30
0.585	153	0.771	0.0241	30
0.585	148	0.767	0.0340	30
0.585	143	0.762	0.0459	30
0.585	138	0.756	0.0596	30
0.585	133	0.750	0.0754	30
0.585	128	0.742	0.0933	30
0.585	123	0.734	0.1134	30

E [GeV]	$\theta$ [°]	q [GeV/c]	$\epsilon$	time [min]
0.585	118	0.724	0.1358	30
0.585	113	0.714	0.1606	30
0.585	108	0.702	0.1880	30
0.585	103	0.689	0.2180	30
0.585	98	0.675	0.2507	30
0.585	93	0.659	0.2861	30
0.585	88	0.642	0.3243	30
0.585	83	0.623	0.3652	30
0.585	78	0.602	0.4087	30
0.585	73	0.580	0.4546	30
0.585	68	0.555	0.5026	30
0.585	63	0.528	0.5523	30
0.585	58	0.499	0.6032	30
0.585	53	0.467	0.6545	30
0.585	48	0.433	0.7054	30
0.585	43	0.397	0.7552	30
0.585	38	0.358	0.8027	30
0.585	33	0.317	0.8471	30
0.585	28	0.273	0.8873	30
0.585	23	0.228	0.9225	30
0.720	158	0.898	0.0151	30
0.720	153	0.894	0.0229	30
0.720	148	0.890	0.0325	30
0.720	143	0.885	0.0438	30
0.720	138	0.879	0.0570	30
0.720	133	0.873	0.0721	30
0.720	128	0.865	0.0893	30
0.720	123	0.856	0.1087	30
0.720	118	0.846	0.1304	30
0.720	113	0.835	0.1546	30
0.720	108	0.823	0.1812	30
0.720	103	0.809	0.2106	30
0.720	98	0.794	0.2427	30
0.720	93	0.777	0.2777	30
0.720	88	0.758	0.3155	30
0.720	83	0.738	0.3562	30
0.720	78	0.715	0.3997	30
0.720	73	0.690	0.4458	30
0.720	68	0.662	0.4943	30
0.720	63	0.632	0.5446	30
0.720	58	0.598	0.5963	30
0.720	53	0.562	0.6486	30
0.720	48	0.523	0.7006	30
0.720	43	0.481	0.7515	30
0.720	38	0.435	0.8001	30
0.855	158	1.011	0.0144	30
0.855	153	1.008	0.0219	30

E [GeV]	$\theta$ [°]	q [GeV/c]	$\epsilon$	time [min]
0.855	148	1.003	0.0310	30
0.855	143	0.998	0.0418	30
0.855	138	0.992	0.0544	30
0.855	133	0.985	0.0690	30
0.855	128	0.977	0.0856	30
0.855	123	0.969	0.1043	30
0.855	118	0.958	0.1252	30
0.855	113	0.947	0.1486	30
0.855	108	0.934	0.1746	30
0.855	103	0.920	0.2032	30
0.855	98	0.904	0.2347	30
0.855	93	0.886	0.2691	30
0.855	88	0.866	0.3065	30
0.855	83	0.845	0.3469	30
0.855	78	0.820	0.3903	30
0.855	73	0.793	0.4365	30
0.855	68	0.763	0.4853	30
0.855	63	0.730	0.5363	30
0.855	58	0.694	0.5888	30
0.855	53	0.654	0.6421	30
0.990	158	1.116	0.0138	30
0.990	153	1.112	0.0209	30
0.990	148	1.108	0.0296	30
0.990	143	1.103	0.0399	30
0.990	138	1.097	0.0521	30
0.990	133	1.090	0.0660	30
0.990	128	1.082	0.0819	30
0.990	123	1.073	0.1000	30
0.990	118	1.063	0.1202	30
0.990	113	1.051	0.1429	30
0.990	108	1.038	0.1681	30
0.990	103	1.023	0.1960	30
0.990	98	1.007	0.2268	30
0.990	93	0.989	0.2606	30
0.990	88	0.968	0.2975	30
0.990	83	0.945	0.3375	30
0.990	78	0.920	0.3807	30
0.990	73	0.891	0.4270	30
0.990	68	0.859	0.4760	30
0.990	63	0.824	0.5275	30
1.125	158	1.214	0.0131	30
1.125	153	1.210	0.0199	30
1.125	148	1.206	0.0283	30
1.125	143	1.201	0.0382	30
1.125	138	1.195	0.0498	30
1.125	133	1.188	0.0632	30
1.125	128	1.180	0.0785	30

E [GeV]	$\theta$ [°]	q [GeV/c]	$\epsilon$	time [min]
1.125	123	1.171	0.0959	30
1.125	118	1.160	0.1155	30
1.125	113	1.149	0.1374	30
1.125	108	1.136	0.1619	30
1.125	103	1.121	0.1891	30
1.125	98	1.104	0.2192	30
1.125	93	1.085	0.2523	30
1.125	88	1.064	0.2886	30
1.125	83	1.041	0.3282	30
1.125	78	1.014	0.3711	30
1.125	73	0.984	0.4173	30
1.260	158	1.306	0.0126	30
1.260	153	1.302	0.0191	30
1.260	148	1.298	0.0271	30
1.260	143	1.293	0.0366	30
1.260	138	1.287	0.0477	30
1.260	133	1.280	0.0606	30
1.260	128	1.272	0.0753	30
1.260	123	1.263	0.0921	30
1.260	118	1.253	0.1110	30
1.260	113	1.241	0.1322	30
1.260	108	1.228	0.1560	30
1.260	103	1.213	0.1825	30
1.260	98	1.196	0.2118	30
1.260	93	1.177	0.2442	30
1.260	88	1.155	0.2800	30
1.260	83	1.131	0.3191	30
1.260	78	1.104	0.3616	30
1.395	138	1.374	0.0458	40
1.395	133	1.367	0.0582	40
1.395	128	1.360	0.0724	30
1.395	123	1.350	0.0885	30
1.395	118	1.340	0.1068	30
1.395	113	1.328	0.1273	30
1.395	108	1.315	0.1504	30
1.395	103	1.300	0.1761	30
1.395	98	1.283	0.2048	30
1.395	93	1.264	0.2365	30
1.395	88	1.242	0.2716	30
1.395	83	1.218	0.3101	30
1.395	158	1.393	0.0120	50
1.395	153	1.390	0.0183	50
1.395	148	1.385	0.0259	50
1.395	143	1.380	0.0351	40
1.530	158	1.476	0.0115	80
1.530	153	1.472	0.0175	80
1.530	148	1.468	0.0249	70

E [GeV]	$\theta$ [°]	q [GeV/c]	$\epsilon$	time [min]
1.530	143	1.463	0.0336	70
1.530	138	1.457	0.0439	60
1.530	133	1.451	0.0559	60
1.530	128	1.443	0.0696	50
1.530	123	1.434	0.0852	50
1.530	118	1.423	0.1028	40
1.530	113	1.412	0.1227	40
1.530	108	1.398	0.1451	30
1.530	103	1.383	0.1701	30
1.530	98	1.366	0.1980	30
1.530	93	1.347	0.2291	30
1.530	88	1.325	0.2635	30
1.530	83	1.300	0.3015	30

## References

- [B<sup>+</sup>98] BLOMQVIST, K. I. et. al.: The three-spectrometer facility at the Mainz microtron MAMI. In: *Nucl. Instrum. Meth. A* **403** (1998) 263–301
- [Ber04] BERNAUER, J. C.: *Vorbereitung zur hochpräzisen Messung des elektrischen und magnetischen Formfaktors von Protonen*, Institut für Kernphysik der Universität Mainz, Diploma thesis, 2004
- [BPS<sup>+</sup>74] BORKOWSKI, F. ; PEUSER, P. ; SIMON, G. G. ; WALTHER, V. H. ; WENDLING, R. D.: Electromagnetic form-factors of the proton at low four- momentum transfer. In: *Nucl. Phys. A* **222** (1974) 269–275
- [CRC04] *Chapter: Subproject H3: Strange Hadrons*. In: CRC 443 "MANY BODY STRUCTURE OF STRONGLY INTERACTING SYSTEMS": *Grand Progress Report 2002-2004*. Institut für Kernphysik der Universität Mainz, 2004
- [Ewa96] EWALD, Ingo: *Entwicklung und Erprobung einer langen, dünnen Flüssig-Wasserstoff-Targetzelle*, Institut für Kernphysik der Universität Mainz, Diploma thesis, 1996
- [FW03] FRIEDRICH, J. ; WALCHER, Th.: A coherent interpretation of the form factors of the nucleon in terms of a pion cloud and constituent quarks. In: *Eur. Phys. J. A* **17** (2003) 607–623
- [G<sup>+</sup>02] GAYOU, O. et. al.: Measurement of  $G(E(p))/G(M(p))$  in  $e(\text{pol.}) p \rightarrow e p(\text{pol.})$  to  $Q^2 = 5.6 \text{ GeV}^2$ . In: *Phys. Rev. Lett.* **88** (2002) 092301
- [GV03] GUICHON, P. A. M. ; VANDERHAEGHEN, M.: How to reconcile the Rosenbluth and the polarization transfer method in the measurement of the proton form factors. In: *Phys. Rev. Lett.* **91** (2003) 142303
- [HMW63] HAND, L. N. ; MILLER, D. G. ; WILSON, R.: Electric and Magnetic Form Factors of the Nucleon. In: *Reviews of Modern Physics* **35** (1963) 335–349
- [Kar99] KARSHENBOIM, Savely G.: What do we actually know about the proton radius? In: *Can. J. Phys.* **77** (1999) 241–266
- [M<sup>+</sup>98] MILBRATH, B. D. et. al.: A comparison of polarization observables in electron scattering from the proton and deuteron. In: *Phys. Rev. Lett.* **80** (1998) 452–455
- [P<sup>+</sup>01] POSPISCHIL, T. et. al.: Measurement of  $G(E(p))/G(M(p))$  via polarization transfer at  $Q^2 = 0.4 \text{ GeV}/c^2$ . In: *Eur. Phys. J. A* **12** (2001) 125–127
- [Ros50] ROSENBLUTH, M. N.: High Energy Elastic Scattering of Electrons on Protons. In: *Phys. Rev.* **79** (1950) 615
- [SSBW80] SIMON, G. G. ; SCHMITT, C. ; BORKOWSKI, F. ; WALTHER, V. H.: Absolute Electron Proton Cross-Sections At Low Momentum Transfer Measured With A High Pressure Gas Target System. In: *Nucl. Phys. A* **333** (1980) 381–391

Further references can be found in [FW03].